Supplementary figures and tables
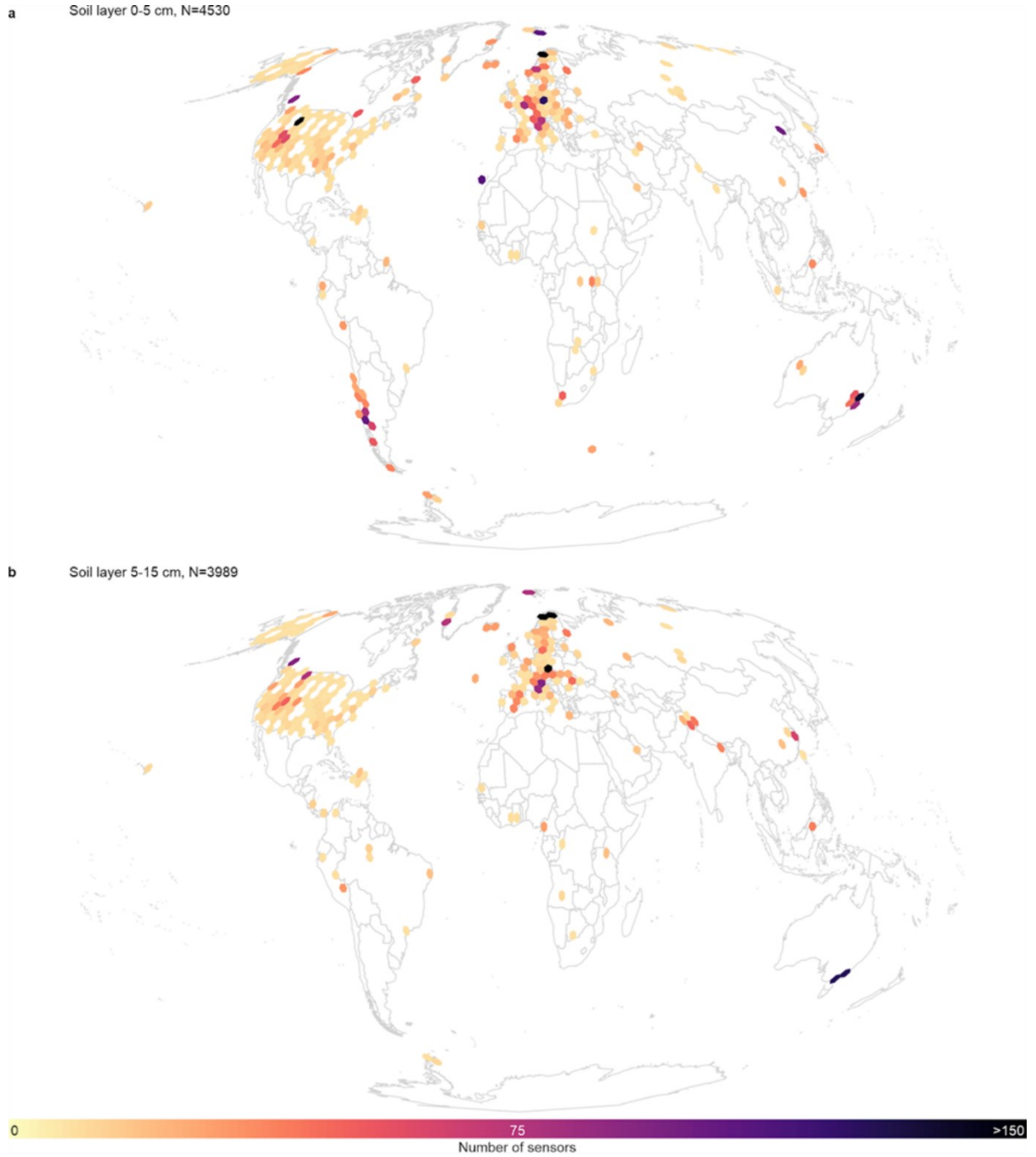

a Soil layer 0-5 cm, N=4530

b Soil layer 5-15 cm, N=3989

0   75   >150
Number of sensors

Fig. S1: Global distribution of the in-situ measurements. Distribution of all sensors in the topsoil (0–5 cm depth, (a), N = 4,530) and the second layer (5–15 cm depth, (b), N = 3,989). Background world map in Mollweide projection, hexagons with a resolution of approximately 70,000 km². Note that sensors appearing here and not in Fig. 1a or Fig. S3 covered time series of less than one year, and thus were only used in the monthly models (see methods for details).
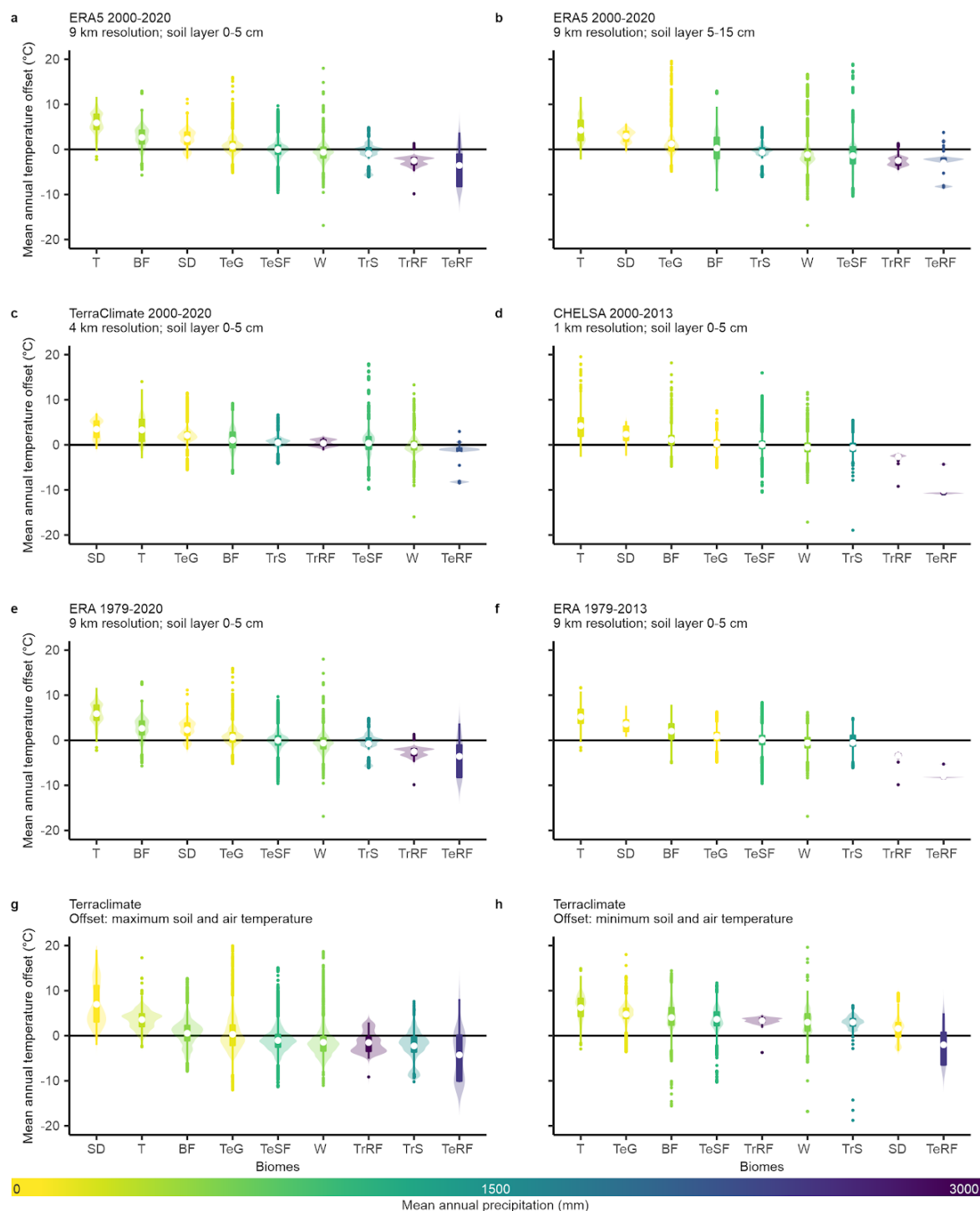
Fig. S2: Annual temperature offsets per biome (as in Fig. 1b), for the first (0–5 cm depth) and second soil layer (5–15 cm depth) and for different air temperature data sources and time periods. Box-and violin plots of the mean annual temperature offsets per Whittaker biome, ordered and coloured by mean annual precipitation. As a standard, we used ERA5L (2000-2020, 9 km resolution) and the topsoil (0–5 cm, (a), see also Fig. 1b). We compare now with the second soil layer (5–15 cm depth, b), with TerraClimate (2000-2020, 4 km resolution, c) and CHELSA (2000-2013, 1 km resolution, d), with ERA5L for the full period (1979-2020, e) and the period matching the

2

bioclimatic variables (1979-2013, f). We also calculate offsets between maximum (95th percentile, g) soil and air temperature, and minimum (5th percentile, h) soil and air temperature, with maximum and minimum air temperature based on TerraClimate. Panels (c) to (h) all use the topsoil data (0–5 cm depth). All panels show relatively consistent results (i.e. strongly positive offsets in tundra, boreal forests, subtropical deserts and temperate grasslands, and weakly negative offsets in tropical savannas and temperate and tropical rainforests). Only annual soil temperature minima were on average higher than corresponding air temperature minima in all but one biomes.
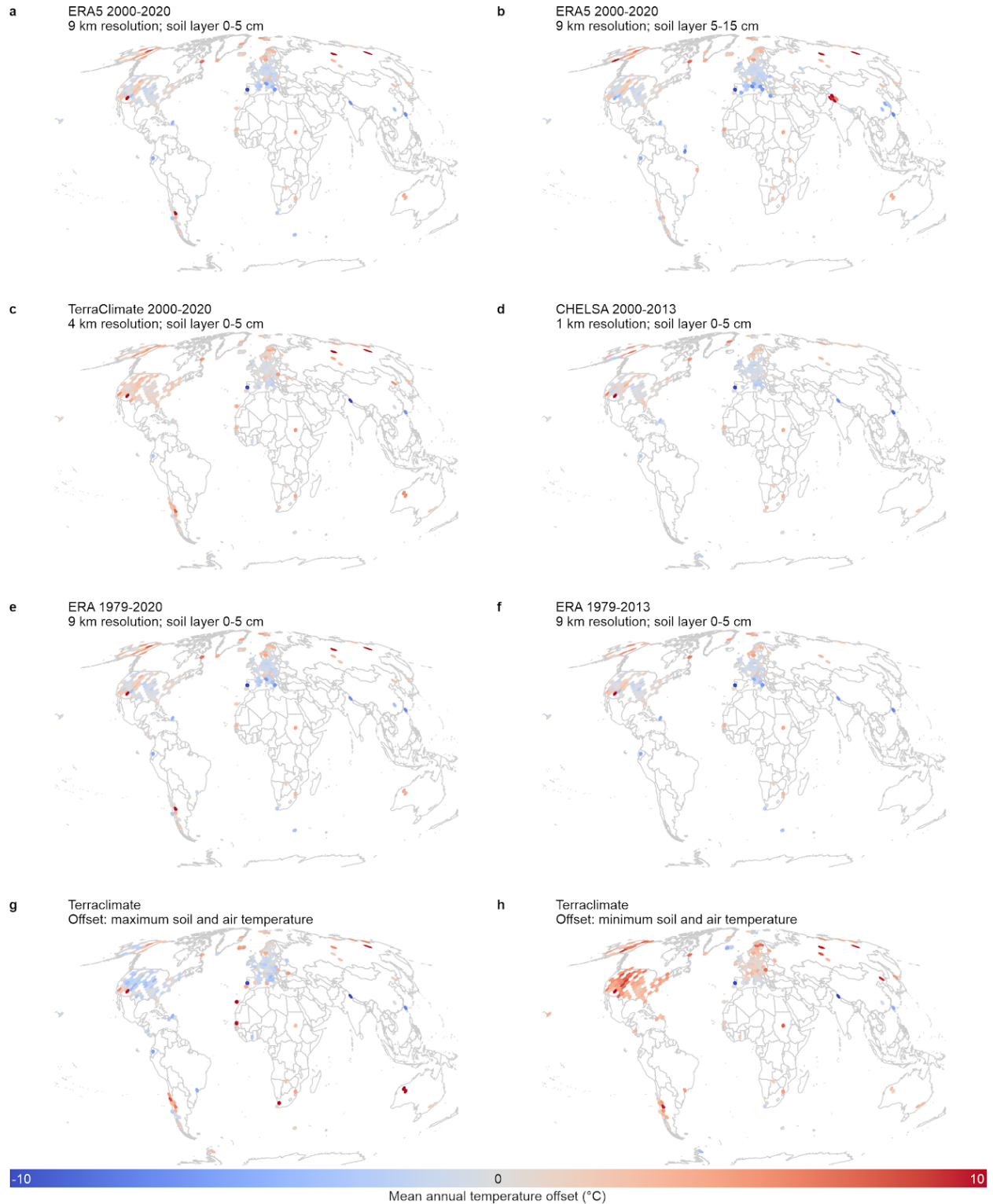
Fig. S3: Annual temperature offset maps (as in Fig. 1a), for the first (0–5 cm depth) and second soil layer (5–15 cm depth), for different air temperature data sources and time periods, and for maximum and minimum temperature. Distribution of sensors across the globe, coloured by the annual offset (in °C) between in-situ measured soil temperature and modelled air temperature. As a standard in Fig. 1a, we used ERA5L (2000-2020, 9 km² resolution) and the

topsoil (0–5 cm, also here in a). We compare now with the second soil layer (5–15 cm depth, b), with TerraClimate (2000-2020, 4 km² resolution, c) and CHELSA (2000-2013, 1 km² resolution, d) for the topsoil layer, and with ERA5L for the full period (1979-2020,e) and the period matching the bioclimatic variables (1979-2013, f). We also calculate offsets between maximum (95th percentile, g) soil and air temperature, and minimum (5th percentile, h) soil and air temperature, with maximum and minimum air temperature based on TerraClimate. Background world map in MollWeide projection, offsets averaged per hexagon with a resolution of approximately 70,000 km², made using the dggridR-package in R. Conclusions about consistency between methods similar as in Fig. S2.
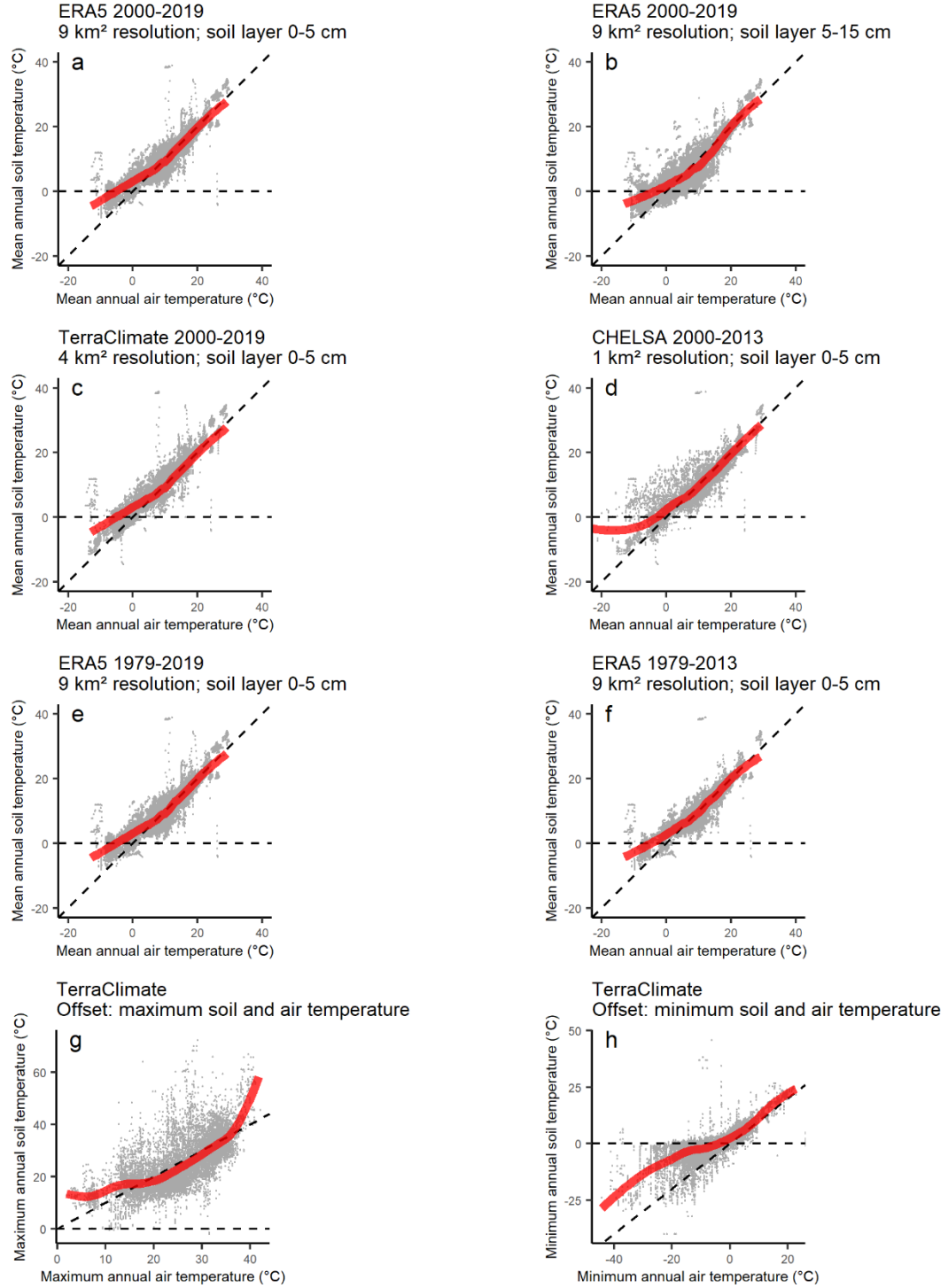
Fig. S4: Relationship between mean annual soil and air temperature at a 1 × 1 km resolution. Point cloud of in-situ mean annual soil temperature (°C) as a function of gridded mean annual air temperature for all in-situ measurements averaged at a 1 × 1 km resolution. As a standard, we used ERA5L (2000-2020, 9 km² resolution) and the topsoil (0–5 cm depth, a). We compare this first with the second soil layer (5–15 cm depth, b). We also compare with analyses for the top soil layer using TerraClimate (2000-2020, 4 km² resolution, c) and CHELSA (2000-2013, 1 km² resolution, d), and with ERA5L for the full period (1979-2020, e) and the period matching the bioclimatic

variables (1979-2013, f). We also plot offsets between maximum (95th percentile, g) soil and air temperature, and minimum (5th percentile, h) soil and air temperature, with maximum and minimum air temperature based on TerraClimate. Straight dashed line indicate a thermal offset of 0°C, and the 1:1-relationship between soil and air temperature, thick red lines the relationship based on generalized additive models, indicating in all cases warmer soil than air temperatures in cold extremes, yet slightly cooler soils at intermediate temperatures (except for h).
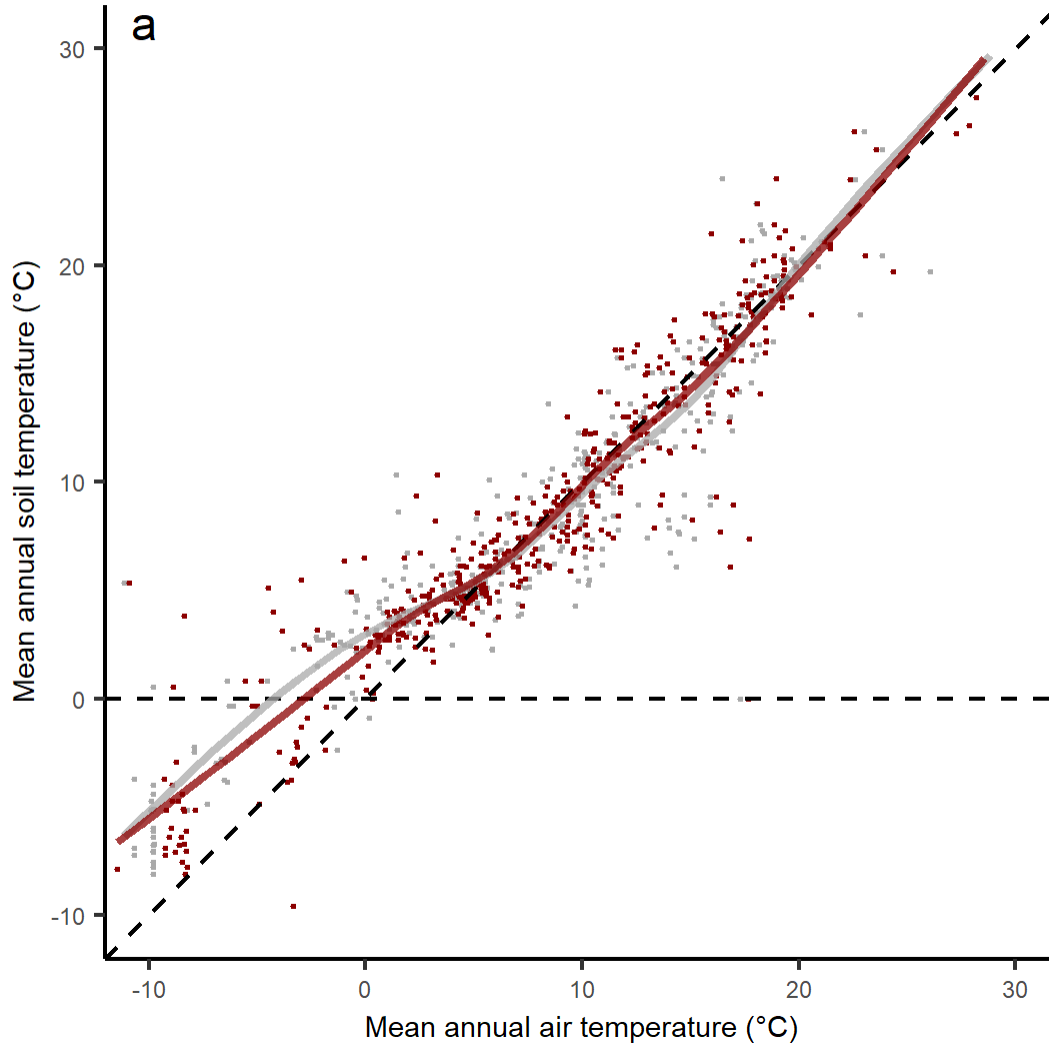
Fig. S5: Relationship between mean annual soil and air temperature for ERA5L (grey) versus CHELSA (red). Point cloud of in-situ mean annual soil temperature (°C) as a function of gridded mean annual air temperature for all in-situ measurements averaged at 1 km², between 2000 and 2013, for ERA5L (grey, 9-km² resolution) and CHELSA (dark red, 1 × 1 km resolution). Straight dashed line indicate a thermal offset of 0°C, and the 1:1-relationship between soil and air temperature, grey and red lines the relationship based on generalized additive models. As in Fig. S4, yet highlighting the strong overlap in pattern when using CHELSA vs ERA5L.
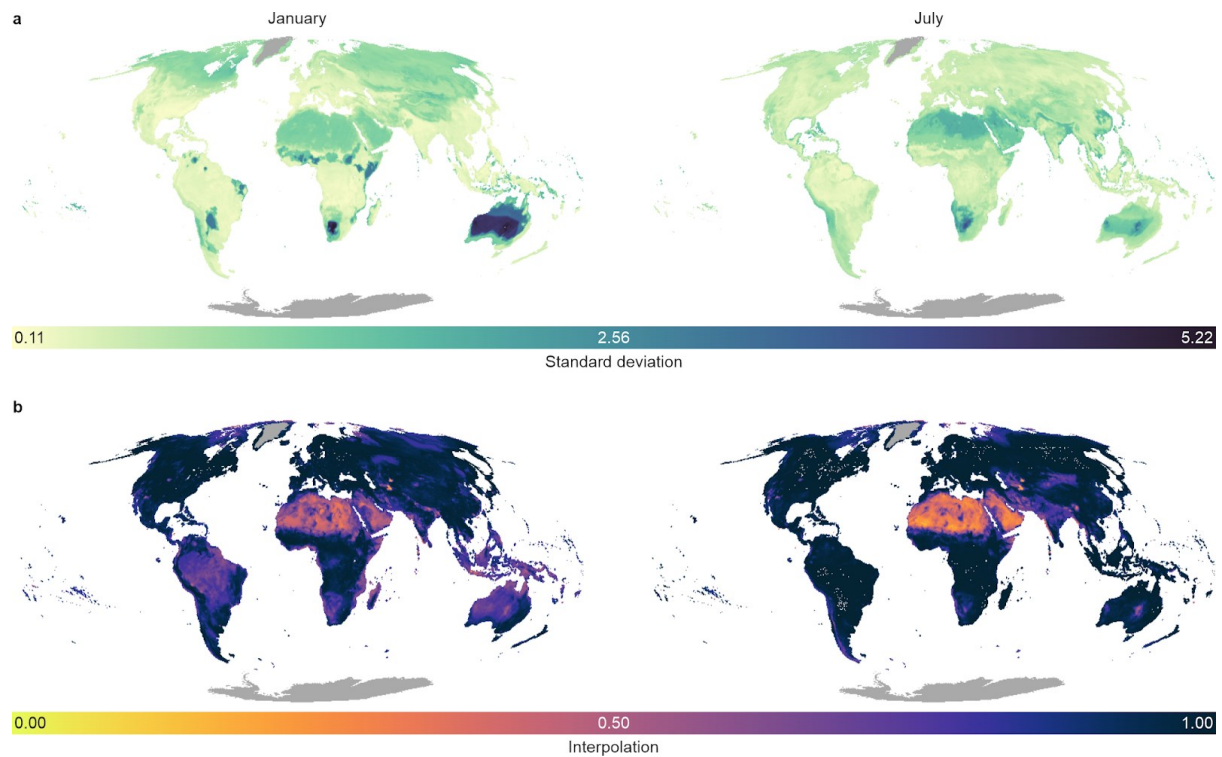
Fig. S6: Predictive performance of the temperature offset models in the second soil layer (5–15 cm depth). Analyses for the temperature offset between in-situ second soil layer (5–15 cm depth) temperature and free-air temperature. (a) Predicted standard deviation from a cross-validation analysis that iteratively varied the set of covariates (explanatory data layers) and model hyperparameters (i.e., number of variables per split; minimum leaf population) across 100 models and evaluated model strength using 10-fold cross-validation, for January (left) and July (right), as examples of the two most contrasting months. (b) The fraction of axes in the multidimensional environmental space for which the pixel lies inside the range of data covered by the sensors in the database. Pixels with low values indicate that the model has to extrapolate for many of the environmental layers for that specific pixel.
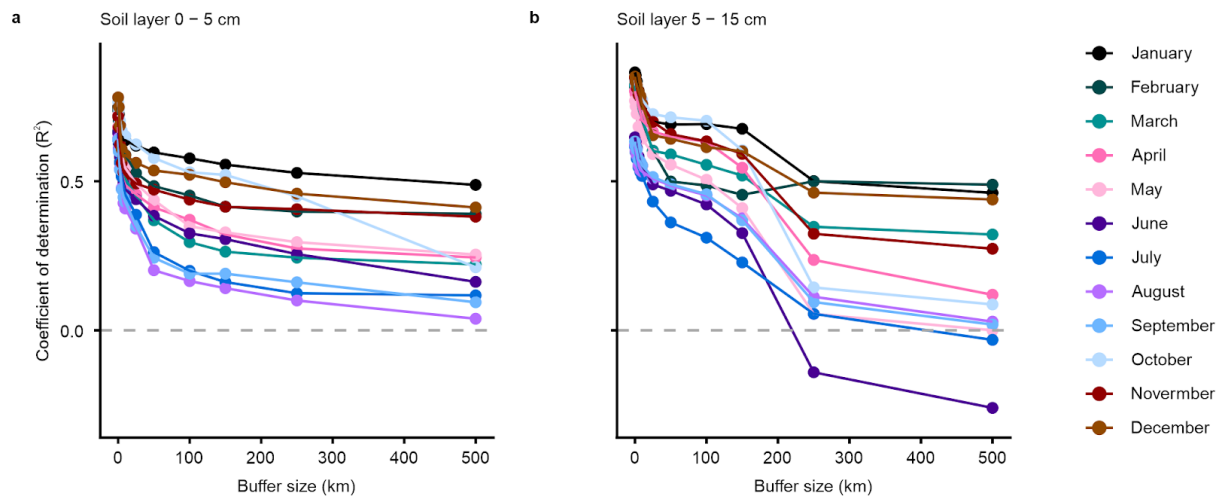
Fig. S7: spatial leave-one-out cross-validation. R² of all monthly models at the two soil depths using a spatial leave-one-out cross validation approach. This approach trains a model for each sample in the dataset on all remaining samples, with an increasingly large buffer around that focal sample. Note that a decrease in R² should be expected with increasing buffer size due to the removal of parts of the environmental gradient from the training dataset. Nevertheless, results show that spatial autocorrelation differs across the months, with uneven global data coverage likely causing lowest confidence for May to September at 5–15 cm depth, where use of data outside of the environmental gradient as covered by the data is thus particularlydiscouraged (see Fig 5b and Fig. S6b).
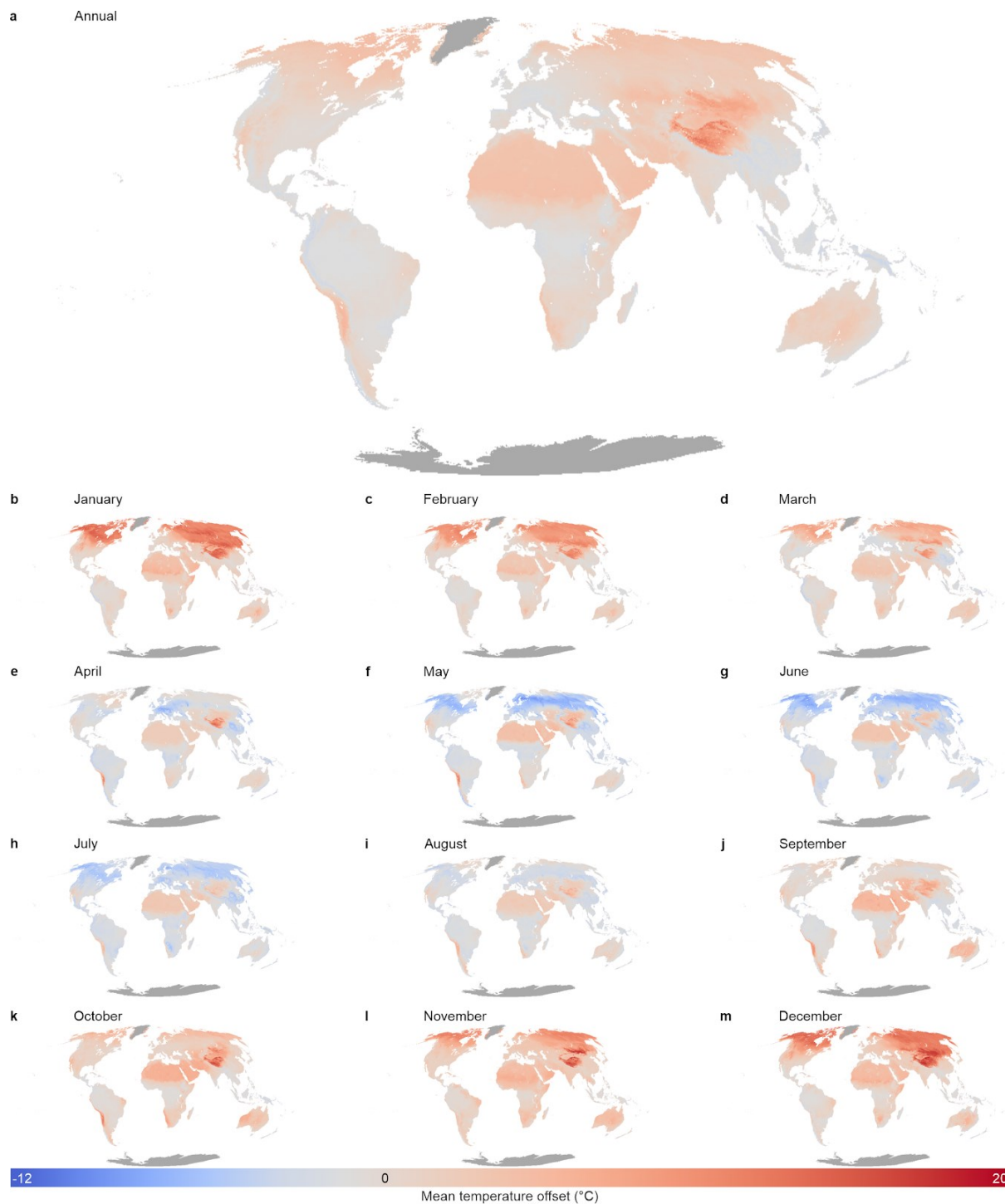
Fig. S8: Modelled mean temperature offset in the second soil layer (5–15 cm depth). Modelled annual (a) and monthly (b-m) temperature offset (in °C) between in-situ measured soil temperature (second soil layer, 5–15 cm depth) and modelled air temperature, in addition to the first soil layer (0–5 cm depth) used in Fig. 2.
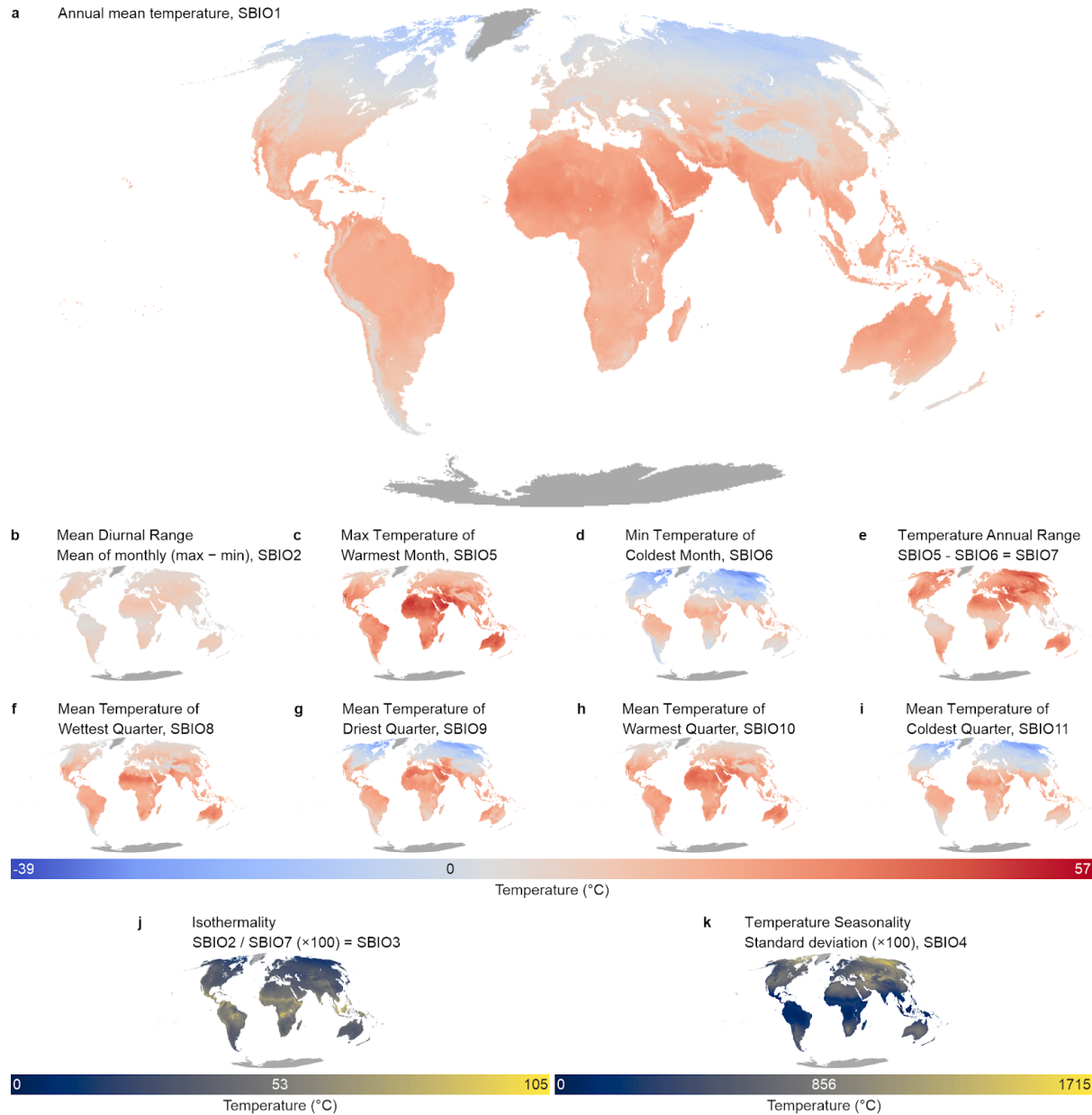
11

a   Annual mean temperature, SBIO1

b   Mean Diurnal Range   **c**   Max Temperature of   **d**   Min Temperature of   **e**   Temperature Annual Range
Mean of monthly (max − min), SBIO2   Warmest Month, SBIO5   Coldest Month, SBIO6   SBIO5 - SBIO6 = SBIO7

f   Mean Temperature of   **g**   Mean Temperature of   **h**   Mean Temperature of   **i**   Mean Temperature of
Wettest Quarter, SBIO8   Driest Quarter, SBIO9   Warmest Quarter, SBIO10   Coldest Quarter, SBIO11

-39   0   57
Temperature (°C)

j   Isothermality   **k**   Temperature Seasonality
SBIO2 / SBIO7 (×100) = SBIO3   Standard deviation (×100), SBIO4

0   53   105   0   856   1715
Temperature (°C)   Temperature (°C)

Fig. S9: Bioclimatic variables for the second soil layer. Global maps of bioclimatic variables for the second soil layer (5–15 cm depth) climate, calculated using the maps of monthly temperature offsets (see Fig. 2, Fig. S8) and the bioclimatic variables for air temperature from CHELSA (*4*).
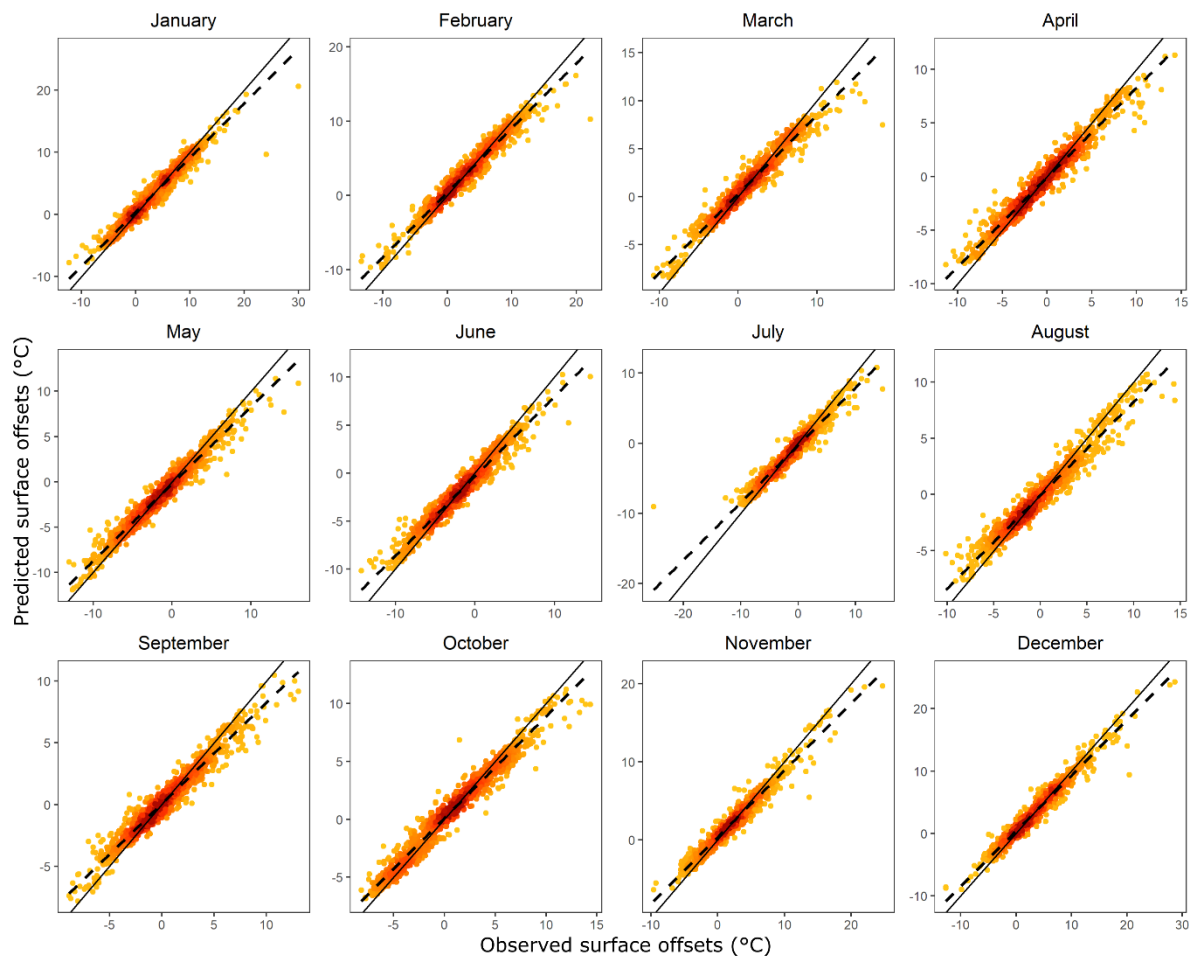
Fig. S10: Observed versus predicted temperature offsets. Correlative plots showing temperature offsets – averaged at a 1 × 1 km resolution – as observed in the field, versus those as predicted by the models, separately for each month. Colours show density of points (darker = higher point density). Dashed lines from linear regressions; solid lines refer to the 1:1-line of perfect correlation between predicted and observed offsets.

Fig. S11: Observed versus predicted temperature offsets per biome. Correlative plots showing temperature offsets – averaged at a 1 × 1 km resolution – as observed in the field, versus those as predicted by the models, separately for each biome, for January (a) and July (b). Colours show density of points (darker = high point density). Dashed lines from linear regressions; solid lines refer to the 1:1-line of perfect correlation between predicted and observed offsets.
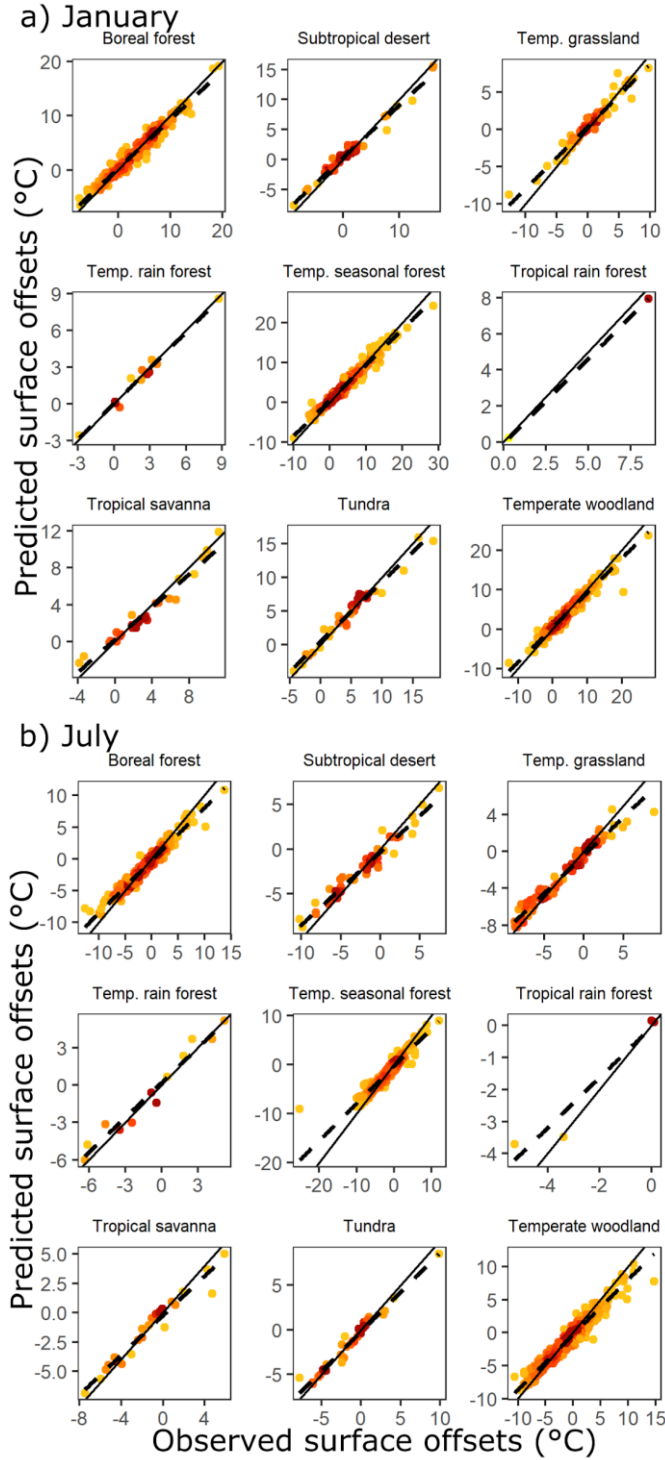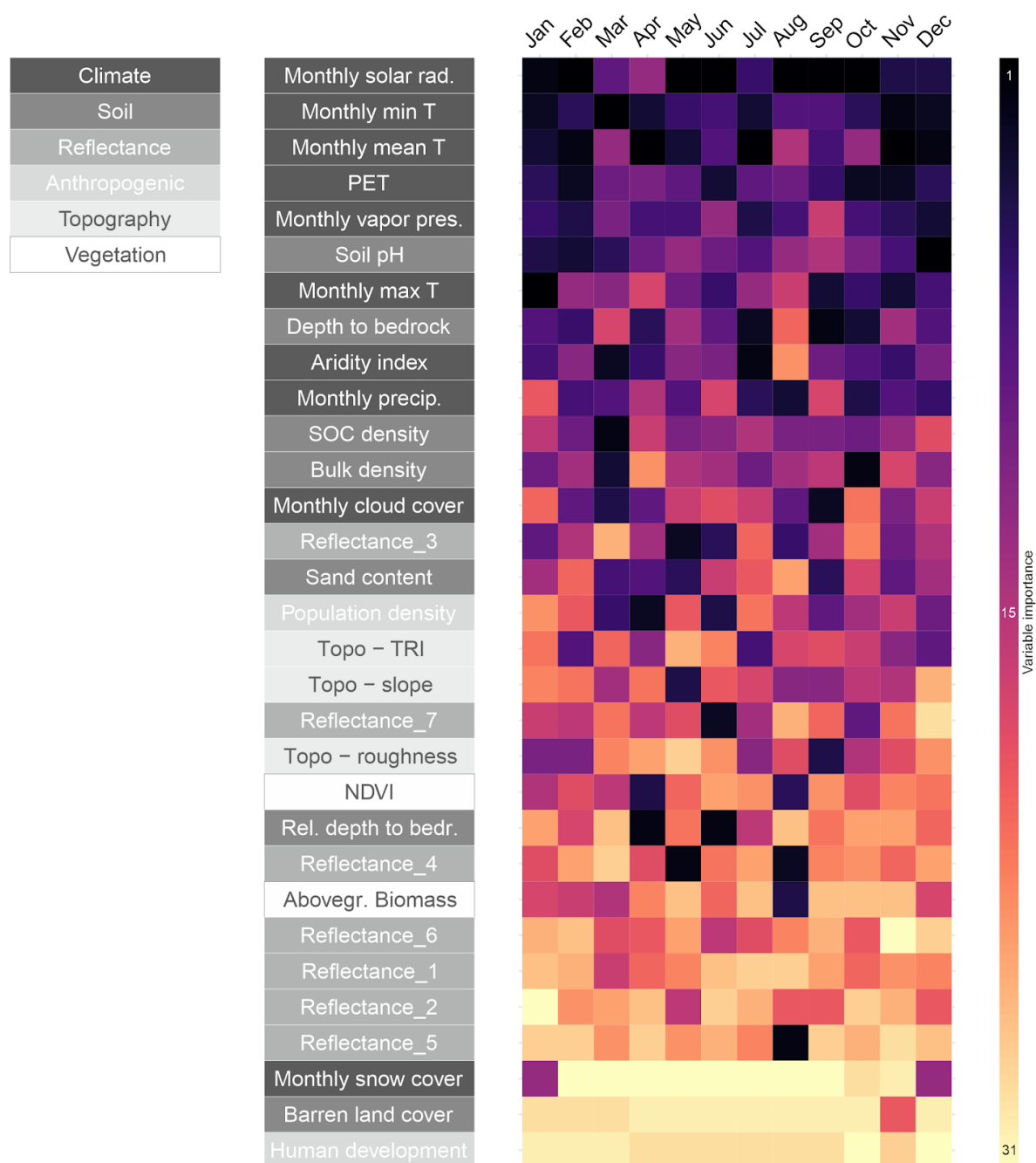
Fig. S12: Relative importance of explanatory variables. Explanatory variables in all twelve monthly analyses sorted by mean Variable Importance (computed based on the summed decrease of impurity over all trees in the forest that results from the variable used at a node; higher for variables with a higher importance) across all models of the first soil layer (0–5 cm depth) (first variable = ranked on average most importantly across all twelve monthly models). Colours represent relative variable importance (ranked from 1 to 31, with 1 the highest importance) within each monthly model for the topsoil (0–5 cm depth). T = temperature, PET = potential evapotranspiration, SOC = soil organic carbon, TRI = topographic roughness index, NDVI = normalized difference vegetation index. For full details on all explanatory variable layers, see Data S1.
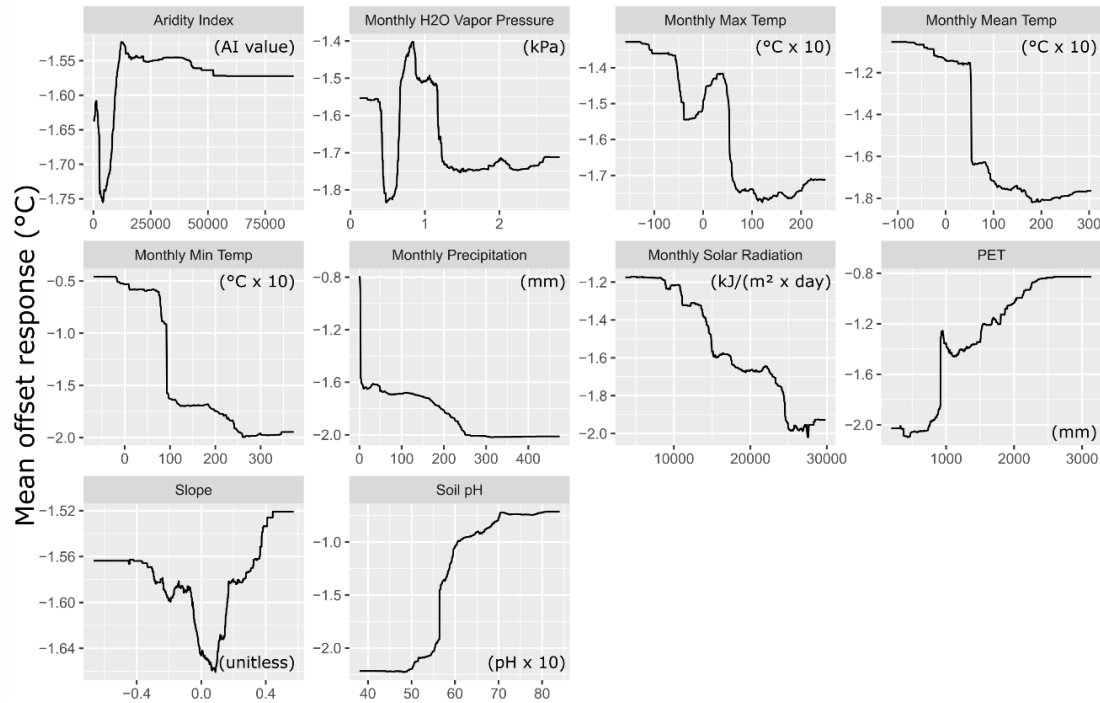
a) January
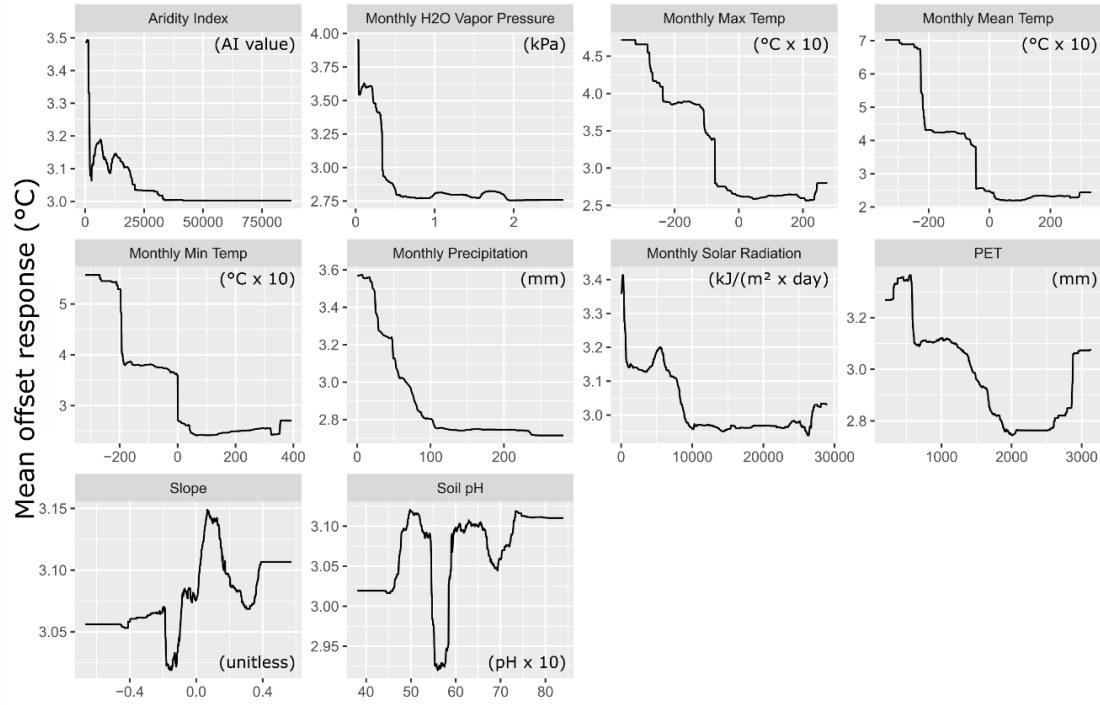
b) July

Fig. S13: Partial dependency plots of main effects. Partial dependency plots of the 10 most important variables (selection based on the mean Feature Importance from Fig. S12) for January (a; top) and July (b; bottom), as examples of the two most contrasting months. Results for the first soil layer (0–5 cm depth)**.**

Supplementary Tables

Table S1: Number of sensors from the most common logger brands in the top soil (left, 0–5 cm depth) and the second soil layer (right, 5–15 cm depth). Other sensors include among others Decagon devices, GeoPrecision data loggers, thermocouples and TinyTags.

Logger brand	Number of sensors	
	0–5 cm	5–15 cm
iButton	1840	1685
TOMST	512	1090
HOBO	689	491
Lascar	247	0
Others	1025	587

Table S2: Number of sensors in each soil layer

Depth of soil layer (cm)	Number of sensors
0–5	4530
5–15	3989
15-30	484
30-60	294
60-100	54
100-200	11

Table S3: Number of data points (in brackets the number of unique pixels after averaging at 1×1 km pixel resolution) for each month as used in the models.

Month	N° of data points (0–5 cm)	N° of data points (5–15 cm)
January	6674 (1212)	10130 (977)
February	6649 (1223)	10214 (986)
March	6527 (1184)	10345 (979)
April	6439 (1093)	10266 (989)
May	6611 (1150)	10510 (1003)
June	6537 (1154)	10546 (1011)
July	6874 (1352)	10515 (1141)
August	6960 (1383)	10950 (1098)
September	6690 (1317)	10484 (1019)
October	6991 (1299)	10429 (1018)
November	6995 (1215)	10683 (996)
December	6846 (1193)	10607 (988)

Table S4: Number of unique pixels after averaging the annual data at 1 × 1 km pixel resolution for each biome, as used in Fig. 1. The number of individual annual averages on which this number is based is shown between brackets.

Biome	N° of pixels (0–5 cm)
Boreal forest	240 (10168)
Sub-tropical desert	37 (802)
Temperate grassland	66 (9558)
Temperate rainforest	10 (27)
Temperate seasonal forest	245 (21566)
Tropical rainforest	2 (299)
Tropical savanna	13 (2062)
Tundra	29 (1584)
Temperate woodland	224 (16952)

Table S5: Number of unique pixels after averaging the monthly data at a 1 × 1 km pixel resolution for each biome as used in the models, averaged across all months.

Biome	N° of pixels (0–5 cm)	N° of pixels (5–15 cm)
Boreal forest	284	323
Sub-tropical desert	46	4
Temperate grassland	82	63
Temperate rainforest	12	2
Temperate seasonal forest	349	304
Tropical rainforest	5	9
Tropical savannah	26	31
Tundra	35	34
Temperate woodland	466	353

Table S6: Biome-specific quantile distribution of the estimated aboveground biomass at the 1 x 1 km pixel level (unit: tons/ha i.e., Mg/ha, for the year 2010, Santoro, 2018) for each sensor identified as either measuring in forests (top) or open vegetation (bottom), for all sensors for which the latter information was available (numbers between brackets). Numbers in green indicate sensors under aboveground biomass of 1.00 tons/ha or higher, here identified as forested.

Biome	1%	5%	25%	50%	75%	95%	99%
Forests							
Boreal forest (18)	53.70	60.50	77.50	84.50	106.00	114.15	114.83
Subtropical desert (3)	2.00	2.00	2.00	2.00	38.00	66.80	72.56
Temperate grassland (12)	3.00	3.00	16.00	45.00	86.00	98.00	98.00
Temperate rain forest (7)	53.12	53.60	63.50	76.00	220.00	296.60	322.52
Temperate seasonal for. (227)	17.00	32.50	63.00	101.00	177.00	291.00	431.00
Tropical rain forest (6)	149.50	167.50	245.50	277.50	284.00	313.75	321.15
Tropical savanna (17)	186.00	186.00	186.00	186.00	207.00	224.00	224.00
Tundra (3)	8.04	8.20	9.00	10.00	12.00	13.60	13.92
Temperate woodland (145)	0.00	0.20	8.00	24.00	120.00	218.00	242.36
Open vegetation							
Boreal forest (463)	0.00	0.00	0.00	0.00	53.00	53.00	105.00
Subtropical desert (13)	0.00	0.00	0.00	0.00	0.00	0.00	0.00
Temperate grassland (44)	0.00	0.00	0.00	0.00	0.00	32.00	107.00
Temperate rain forest (0)	-	-	-	-	-	-	-
Temperate seasonal for. (89)	0.00	0.00	0.00	0.00	32.00	223.00	248.08
Tropical rain forest (0)	-	-	-	-	-	-	-
Tropical savanna (0)	-	-	-	-	-	-	-
Tundra (75)	0.00	0.00	0.00	0.00	0.00	6.00	10.00
Temperate woodland (93)	0.00	0.00	1.00	19.00	66.00	171.00	172.00

Table S7: Difference in temperature offset between forested and unforested habitats. Mean and standard deviation of offsets per Whittaker biome for all sensors, and for sensors in forested and non-forested habitats separately. All values averaged at a 1×1 km resolution (number between brackets = number of unique 1×1 km pixels), only biomes with sufficient number of loggers in forested habitats are shown. Habitat assessment at the location of the sensor based on observations by the contributors, whenever available (60% of sensors).

Biome	All	Forested	Non-forested
Boreal forest	2.47 ± 2.01 (240)	3.40 ± 1.64 (41)	3.12 ± 1.77 (105)
Temperate grasslands	0.92 ± 2.13 (66)	1.39 ± 2.79 (4)	1.30 ± 2.79 (27)
Temperate seasonal forests	0.46 ± 2.79 (245)	-0.82 ± 2.21 (53)	1.00 ± 3.95 (20)
Temperate woodland	-0.12 ± 3.38 (224)	-0.71 ± 3.11 (31)	1.22 ± 4.31 (35)

Data S1. (separate file)

Final selection of global covariate layers used for geospatial modelling. A total of 31 global covariate layers was used in our modelling approach.